F12+EOM Quartic Force Fields for Rovibrational Predictions of Electronically Excited States

Megan C. Davis, Noah R. Garrett, and Ryan C. Fortenberry*

Department of Chemistry & Biochemistry, University of Mississippi, University, MS, 38677-1848, USA

E-mail: r410@olemiss.edu

Abstract

Quartic force fields (QFFs) constructed using a sum of ground-state CCSD(T)-F12b energies with EOM-CCSD excitation energies are proposed for computation of spectroscopic properties of electronically excited states. This is dubbed the F12+EOM approach and is shown to provide similar accuracy to previous methodologies at lower computational cost. Using explicitly correlated F12 approaches instead of canonical CCSD(T), as in the corresponding (T)+EOM approach, allows for 70-fold improvement in computational time. The mean percent difference between the two methods for anharmonic vibrational frequencies is only 0.10%. A similar approach is also developed herein which accounts for core correlation and scalar relativistic effects, named F12cCR+EOM. The F12+EOM and F12cCR+EOM approaches both match to within 2.5% mean absolute error of experimental fundamental frequencies. These new methods should help in clarifying astronomical spectra by assigning features to vibronic and vibrational transitions of small astromolecules when such data is not available experimentally.

Introduction

Ab initio spectroscopic modelling of electronically excited states would aid in clarifying astronomical spectra potentially leading to the discovery of new molecules in space.[1–4] Other applications include providing complete partition functions to molecules in highly energetic environments, enhancing a complete understanding of photophysics needed for solar energy harvesting, and characterizing species involved in charge-transfer reactions to name a few. An immediate planetary science application would be in the classification of cometary spectra. Such spectra include numerous electronic transitions originating from the ion tail[5,6] that are not fully correlated with their molecular or atomic carriers. Additionally, assigning features to vibronic or vibrational transitions of electronically excited states of already known astromolecules would aid in identification of novel molecules whose spectra may be otherwise clouded,[7] thereby "pulling the weeds" of astronomical spectra.

The James Webb Space Telescope (JWST), which began its scientific mission within the past year, provides the scientific community with high resolution spectra ranging from 0.7 microns all the way to 30 microns effectively encapsulating the entire range of vibrational transition wavelengths. Consequently, modelling the rovibrational transitions of electronically excited states would be useful in clarifying spectra in this range as well as long-wavelength electronic transitions. Additionally, observations from the ground or with the Hubble Space Telescope in the ultraviolet and visible ranges are also ongoing and would be greatly enhanced by having rovibronic spectral benchmarks for molecules of interest. Thus, providing rotational and vibrational spectroscopic data for electronically excited states would allow for more accurate models of astronomical spectra *in silico*. Many of the needed observables, such as vibrationally corrected rotational constants, are difficult to experimentally characterize. Therefore, theory is necessary to provide full model spectra.

Quartic force fields (QFFs) based on coupled cluster theory[8–10] are capable of providing high level rovibrational characterization of ground electronic states.[11,12] QFFs using canonical coupled cluster singles, doubles, and perturbative triples [CCSD(T)] routinely achieve

accuracy of within 5 cm^{-1} for fundamental vibrational frequencies and 20 MHz for rotational constants relative to experiment.[11,13–24] Explicitly correlated F12-based approaches[25,26] can achieve similar or better accuracy for substantially less computational cost due to the use of small explicitly correlated basis sets[27–30] making these more recent advancements in chemical theory the next natural means of advancing QFF results.

However, these methods may not be applied to electronic configurations other than the ground state, except in cases where the target state is variationally accessible.[31,32] Thus, QFFs based on electronically excited state methods are necessary to compute spectroscopic parameters for these higher-energy states. The equation of motion (EOM) formalism extends coupled cluster theory and its benefits–e.g. a "black box" approach and hierarchal convergence–to electronically excited states in a relatively robust manner.[33] Thus, exploring EOM-based approaches is an obvious direction to extend QFFs to electronically excited states. EOM-CCSD energies, though, do not exhibit high-enough levels of correlation for spectroscopic accuracy.[34,35] In order to bring EOM-based QFFs closer to the level of accuracy produced with ground-state type approaches, some form of perturbative triples correction in the least is necessary. Furthermore, avoiding inordinate computational cost is essential for treating any but the smallest molecular systems.[17,31]

The so-called (T)+EOM QFFs[36] achieve accuracy compared to ground electronic state type benchmarks for a small set of triatomic test cases–within 1.6 cm^{-1} for one species–and, thus, seem to be a promising avenue of exploration. A (T)+EOM QFF accounts for some triples correction by approximating the total energy of the target state as a sum of a ground state CCSD(T) reference energy and an EOM-CCSD excitation energy from the reference state to the target electronic state of interest. This composite nature makes (T)+EOM calculations trivial to actualize with existing quantum chemistry codes. However, the best (T)+EOM method relies on expensive quintuple-zeta basis set calculations, limiting its applicability beyond small systems. Of additional concern is the need for further benchmarking of the approach for more test cases.

A straightforward way to improve upon the (T)+EOM approach would be to base its reference state component on explicitly correlated CCSD(T)-F12 energies rather than canonical CCSD(T) ones. This allows for substantial reduction in basis set size without sacrificing computational accuracy, eliminating the need for a costly complete basis set extrapolation[12] and approximating a quintuple basis set level quality with substantially less expensive triple-zeta level computations.[37] Explicitly-correlated methods have been successfully used to construct QFFs with drastically decreased computational cost for ground electronic states,[27–30] and the extension of these to treat electronically excited states should make electronically excited state QFFs more feasible.

Thus, in order to build upon the work presented in Ref. 36 by developing a similar methodology with reduced cost, the present work shall herein define and test "F12+EOM" QFFs–e.g. electronically excited state QFFs which utilize reference-state CCSD(T)-F12 energies with EOM-CCSD excitations to a target state. Ground state QFFs based purely on CCSD(T)-F12 energies without further corrections are accurate for vibrational frequencies but do not quite achieve spectroscopic accuracy for rotational constants.[24] This is ameliorated by approaches which include corrections for core electron correlation and scalar relativistic effects.[30] As a result, such an approach is likely feasible for (T)+EOM-type QFFs based on F12 energies.

The test set of molecules used to evaluate the F12+EOM approach uses the following criteria. The molecules should have as few atoms as possible so that multiple benchmark QFFs may be performed. They should also have a variety of atoms reflecting those for the desired application, mainly p-block elements in this case. They should also have a variety of chemical bonds and available experimental data for vibrational frequencies. Additionally, the test set should include open-shell species, as these make up many electronic states of interest.[38,39] Linear molecules are avoided in the present study in order to avoid complications with Renner-Teller effects.[17,40] The test cases are also selected based on astronomical interest, in keeping with the principle astrochemical motivation outlined previously, as this

would provide immediately useful data to the astrochemistry community. Species with relatively high column densities in the interstellar medium[41] make for good candidates of study, since work providing the full set of spectroscopic data for electronically excited states of these species could prove useful for future astrochemical applications. Such species include HNCO,[24] HNO, HSS,[21,42] and HOO.[22] Low lying radicals, aside from being of astronomical interest[41] also allow for variational treatment of ground-state type QFFs providing further benchmarking with established methods. Experimental benchmarks for vibrational frequencies are gathered using gas phase data cited in the NIST database.[43]

Theory-to-theory benchmarking is done in two ways. The first is by comparing the F12+EOM family of approaches directly with the previous (T)+EOM/CcCR approach for the entire test set. Secondly, three types of ground-state benchmark quartic force fields are also used for comparison for molecules which have variationally accessible electronically excited states. Both the F12+EOM and (T)+EOM/CcCR approaches are compared against these ground-state type benchmarks. Theory-to-experiment comparisons are made for the F12+EOM family and (T)+EOM/CcCR approaches for all experimentally known vibrational modes of the electronically excited states in the test set. Comparisons are made based on the mean absolute errors of vibrational frequencies for theoretical and experimental benchmarks, as well as for rotational constants for theoretical benchmarks.

Computational Methods

Eq 1 gives the molecular Watson Hamiltonian. The potential term V(Q) can be efficiently approximated with a fourth-order Taylor series expansion (Eq 2). This is known as a QFF. Once the QFF is formed, second-order vibrational perturbation theory (VPT2) may be used to compute spectroscopic data for a given system.

$$H = \frac{1}{2}\sum_{\alpha\beta}(J_\alpha - \pi_\alpha)\mu_{\alpha\beta}(J_\beta - \pi_\beta) - \frac{1}{2}\sum_k \frac{\partial^2}{\partial Q_k^2} - \frac{1}{8}\sum_\alpha \mu_{\alpha\alpha} + V(Q). \quad (1)$$

$$V = \frac{1}{2}\sum_{ij} F_{ij}\Delta_i\Delta_j + \frac{1}{6}\sum_{ijk} F_{ijk}\Delta_i\Delta_j\Delta_k + \frac{1}{24}\sum_{ijkl} F_{ijkl}\Delta_i\Delta_j\Delta_k\Delta_l \quad (2)$$

The first step in computing a QFF is to obtain an optimized geometry at a given level of theory using tight convergence criteria. This is used as the reference geometry, which is then displaced along symmetry internal coordinates at a step size of 0.005 Å or radians. A single point energy is computed at the given level of theory for each of these geometries. These energies then undergo a least squares fitting to the Taylor series function, generating a set of force constants in symmetry internal coordinates. The geometry is then refit to the exact minimum and a new set of force constants is generated. These force constants are then converted to Cartesian coordinates. The Cartesian force constants are then fed into the program SPECTRO[44] to generate spectroscopic data with VPT2[44–46] while taking into account Fermi and Coriolis resonances and polyads.[47] Further detail concerning QFF construction may be found in Ref. 11.

The eight test cases used for the present study include four radicals: $\tilde{\text{A}}\ ^2A'$ HNF, $\tilde{\text{A}}\ ^2A'$ HSO, $\tilde{\text{A}}\ ^2A'$ HSS and $\tilde{\text{A}}\ ^2A'$ HOO. These species are studied with both ground-state type QFFs and electronically excited state QFFs. Treating these species with ground-state type QFFs is possible because these states are variationally accessible.[31,32] This is done simply by specifying the correct symmetry of the electronic wavefunction when computing energies. The ground-state type QFFs thus provide benchmarking for the purely electronically excited state QFFs to be defined in detail below. Four additional species studied herein are $\tilde{\text{A}}\ ^1A''$ HNO, $\tilde{\text{A}}\ ^1A''$ HCF, $\tilde{\text{A}}\ ^1B_1$ NH_2 and $\tilde{\text{A}}\ ^1A''$ HNCO (isocyanic acid) chosen for their availability of experimental data and to represent additional types of bonds. Restricted open-shell Hartree-Fock (ROHF) is used for all open-shell computations.

Defining ground-state benchmark approaches first, an F12-TZ QFF[27–29] uses CCSD(T)-F12b/cc-pVTZ-F12 for the optimized geometry and single point energies. The related F12-TZ-cCR approach[30] uses the CCSD(T)-F12b method with core electron correlation and the cc-pCVTZ-F12 basis set[48] along with an additional scalar relativistic correction using

the Douglas-Kroll formalism within canonical CCSD(T).[49,50] A final benchmark QFF uses canonical CCSD(T) energies with a three-point complete basis set extrapolation[47] using aug-cc-pVXZ (X=T,Q,5) basis sets[51–53] together with additive corrections for core correlation using the Martin Taylor basis set[54] and Douglas-Kroll scalar relativistic corrections. This is known as the "CcCR" approach.[24,55] CcCR QFFs use a reference geometry computed at the CCSD(T)/aug-cc-pV5Z level of theory with a Martin-Taylor core correlation correction to the geometrical parameters.

The (T)+EOM family of approaches[36] uses the scheme given in Eq. 3 for targeting electronically excited states. The total (T)+EOM energy of the target state at a given geometry is defined as the sum of the ground-state CCSD(T) energy of a reference state (i.e. the ground electronic state) and the EOM-CCSD *excitation energy* from the reference state to the ground state. These excitation energies are computed using the equation-of-motion excitation energy (EOMEE) variant of EOM for all molecules in the present study. The composite (T)+EOM energy may be numerically optimized to obtain a reference geometry for the QFF. The (T)+EOM/CcCR approach is analogous to the ground state CcCR approach defined above, where (T)+EOM energies for a target state are used instead of canonical CCSD(T) energies. The (T)+EOM/CcCR reference geometry is obtained according to Eq. 4. This reference geometry is formed as a sum of geometrical parameters obtained at the (T)+EOM/aug-cc-pV5Z level of theory and an additive correction constructed from (T)+EOM energies using the Martin-Taylor basis set with (MTc) and without (MT) core correlation. Eq. 5 defines the single-point energies used in a (T)+EOM/CcCR QFF. The single-point energy term consists of a (T)+EOM formed from a three-point basis set extrapolation and additive corrections for core correlation and scalar relativistic effects.

$$E_{\text{(T)+EOM}} = E^{GS}_{\text{CCSD(T)}} + E^{XS}_{\text{EOM-CCSD}} \tag{3}$$

$$R_{(T)+EOM/CcCR} = R_{(T)+EOM/aug-cc-pV5Z} + (R_{(T)+EOM/MTcore} - R_{(T)+EOM/MT}). \quad (4)$$

$$E_{(T)+EOM/CcCR} = E_{(T)+EOM/CBS} + \Delta E_{(T)+EOM/MTcore} + \Delta E_{(T)+EOM/DKrel}. \quad (5)$$

Members of the F12+EOM family build upon the fundamental approach of the (T)+EOM QFFs. The difference between the two is that F12+EOM QFFs use CCSD(T)-F12b energies for the reference state energies, rather than canonical CCSD(T) as in the (T)+EOM family, i.e.:

$$E_{\text{F12+EOM}} = E^{GS}_{\text{CCSD(T)-F12b}} + E^{XS}_{\text{EOM-CCSD}} \quad (6)$$

The aim of this approach is to reduce computational cost by lowering the necessary basis set size for accurate computations using CCSD(T)-F12b energies. The F12+EOM-TZ QFF is thus defined as follows, using triple-zeta quality basis sets:

$$E^{XS}_{\text{F12+EOM}} = E^{GS}_{\text{CCSD(T)-F12b/cc-pVTZ-F12}} + E^{XS}_{\text{EOM-CCSD/aug-cc-pVTZ}}. \quad (7)$$

The above equation also defines the energy which is optimized to obtain the reference geometry for the F12+EOM-TZ QFF. Additionally, the F12+EOM-DZ QFF is tested in this work. This QFF is constructed in the same way as the F12+EOM-TZ QFF but uses double-zeta quality basis sets instead of triple-zeta.

A final F12+EOM QFF is constructed by using core correlating basis sets (cc-pCVTZ-F12 for the CCSD(T)-F12b energy term and aug-cc-pcVTZ for the EOM-CCSD term) with an unfrozen core. The addition of a Douglas-Kroll scalar relativistic correction computed using the cc-pVTZ-DK basis set forms what is known as the F12cCR+EOM. The Douglas-Kroll correction is computed using a (T)+EOM energy rather than an F12+EOM energy. The reference geometry for the F12cCR+EOM is obtained by optimizing the $E_{\text{F12+EOM/cc-pcVTZ-F12}}$

energy with an unfrozen core.

$$E_{\text{F12cCR+EOM}} = E_{\text{F12+EOM/cc-pcVTZ-F12}} + \Delta E_{\text{(T)+EOM/DKrel}}. \quad (8)$$

Table 1 summarizes the computational methods used in this paper.

Table 1: Summary of QFFs Used. MTc = Martin Taylor core correlation correction; DKr = Douglas Kroll scalar relativistic correction

Category	Method	Base Energy	Additive Corrections
Ground-state	CcCR	CCSD(T)/CBS(T-Q-5)	ΔCCSD(T)/DKr + ΔCCSD(T)/MTc
	F12-TZ	CCSD(T)-F12b/cc-pVTZ-f12	n/a
	F12-cCR-TZ	CCSD(T)-F12b/cc-pCVTZ-F12	ΔCCSD(T)/DKr
Excited-state	(T)+EOM/CcCR	(T)+EOM/CBS(T-Q-5)	Δ(T)+EOM/DKr + Δ(T)+EOM/MTc
	F12+EOM-TZ	F12+EOM/(cc-pVTZ-f12/aug-cc-pVTZ)	n/a
	F12+EOM-DZ	F12+EOM/(cc-pVDZ-f12/aug-cc-pVDZ)	n/a
	F12cCR+EOM	F12+EOM/(cc-pCVTZ-F12/aug-cc-pCVTZ)	Δ(T)+EOM/DKr (core included in base energy)

Adiabatic excitation energies (AEE) are estimated for the F12+EOM, F12cCR+EOM, and (T)+EOM QFFs by taking the total energy of the electronically excited state at a given level theory at the minimum geometry and subtracting the energy of the corresponding ground-state QFF (e.g. F12-TZ, F12-TZ-cCR, or CcCR) at the minimum geometry for the ground electronic state. These energies are further corrected by the computed VPT2 zero point energy and refitting energy, high-level estimations of the excitation energy.

Energies and optimized geometries for CcCR, F12-TZ and F12-TZ-cCR QFFs are computed using MOLPRO 2020.[56] (T)+EOM/CcCR, F12+EOM and F12cCR+EOM QFFs are computed using MOLPRO for closed-shell states. QFFs for open-shell electronically excited states are computed using MOLPRO for CCSD(T) or CCSD(T)-F12b energies and PSI4[57] for open-shell EOM-CCSD energies. Optimized geometries are obtained for these cases by separately computing the numerical gradients and feeding them into a geometry optimization wrapper script. An additional caveat is that, for open-shell species, scalar relativistic corrections are only applied to the ground state portion of a (T)+EOM or F12+EOM energy, as the Douglas-Kroll formalism is implemented in MOLPRO but not in PSI4. This is not expected to affect the QFFs significantly as the Douglas-Kroll correction typically

amounts to a change of a few wavenumbers at most for fundamental anharmonic vibrational frequencies.[14] Future work may involve the choice of a separate scalar relativistic correction such as the exact two-component approach.[58]

Results

Experimental benchmarks

Table 2: Mean Absolute Differences of Electronically Excited State QFF Vibrational Frequencies and Adiabatic Excitation Energies to Experimental Values in cm^{-1}

	F12+EOM-DZ		F12+EOM-TZ		F12cCR+EOM		(T)+EOM/CcCR	
	MAE v	Δ AEE	MAE v	Δ AEE	MAE v	Δ AEE	MAE v	Δ AEE
A $^2A'$ HOO [a]	129.6	330.0	125.6	56.5	132.6	49.7	126.4	152.0
A $^2A'$ HNF [b]	11.0	514.6	12.2	260.4	12.6	192.1	13.7	9.0
A $^1A''$ HCF [c]	13.6	426.1	13.7	144.0	17.5	24.9	12.3	47.0
A $^1A''$ HNO [d]	38.7	393.0	38.8	38.8	44.3	44.3	45.8	45.8
A $^2A'$ HSO [e]	1.9	6.0	13.7	198.7	11.9	142.7	16.1	113.4
A $^2A'$ HSS [f]	29.1	135.1	23.7	81.3	22.3	126.9	25.9	60.9
A $^1A''$ HNCO [g]	24.5	368.8	30.8	631.5	32.4	904.3	29.3	1059.3
average	35.5	310.9	36.9	201.6	39.1	212.1	38.5	212.5

[a] Refs 59–61; [b] Refs 62,63; [c] Refs 64–68
[d] Refs 69,70; [e] Refs 71; [f] Refs 72–74
[g] Refs 75,76

Experimental data are available for many of the vibrational frequencies of the chosen test cases as well as for adiabatic excitation energies (AEEs). Table 2 gives mean absolute errors (MAE) relative to experimental values. F12+EOM-DZ surprisingly compares the best to experiment out of the current set of QFFs, with an overall MAE of 35.5 cm^{-1}. F12+EOM-TZ performs similarly with an overall MAE of 36.9 cm^{-1}, and F12cCR+EOM is close behind at 39.1 cm^{-1}. (T)+EOM/CcCR achieves an MAE of 38.5 cm^{-1}, a similar performance to the F12+EOM family. Looking at the individual species in Table 2, F12+EOM-DZ MAEs are closest to experiment for all molecules except HOO and HSS. F12+EOM-DZ is particularly close for HSO, with an MAE of only 1.9 cm^{-1}. As a word of caution, summary statistics of data gathered from many different experiments as is done here paint with a somewhat broad

brush. Thus, exact frequencies computed herein and those gathered from experimental work are collected in the Supplementary Information for the interested reader. The MAE metric is chosen for this discussion rather than a normalized comparison of fundamental frequencies. Comparing relative rather than absolute error could mask larger discrepancies of band origin predictions in higher-frequency vibrations and thus exaggerate performance.

The major outlier for experimental comparisons is HOO, and agreements with experiment are considerably closer across the board for the remaining set of molecules. Experimental data for HOO disagrees significantly with all levels of theory for the H-O stretch and to a lesser extent the O-O stretch as discussed in previous work.[36] This may represent a potential flaw with the QFF approach applied to HOO in general rather than flaws with these particular excited state approaches since ground-state type QFFs are generally in line with the (T)+EOM and F12+EOM-TZ results, as discussed in the below section on theoretical benchmarks. The ν_3 frequency agrees much more closely with the computed values for all QFFs. This is given in Table S1.

Turning to AEEs, an overall reasonable agreement with experimental values is produced for F12+EOM-TZ and F12cCR+EOM, with an average of 201.6 cm^{-1} (2.4%) and 212.1 cm^{-1} (2.5%) for F12+EOM-TZ and F12cCR+EOM. In particular, AEEs match exceptionally well for HNO and HOO for F12+EOM-TZ. F12cCR+EOM does a better job of modelling HCF, with a difference of only 24.9 cm^{-1} (0.14%). The biggest outlier is HNCO, followed by HNF. This is to be expected as these states have the largest excitation energies with experimental values of 32440 cm^{-1} [75,76] and 20140 cm cm^{-1},[63] respectively. Thus, a similar percent error will result in a larger difference for these states. Interestingly, F12+EOM-DZ underperforms for AEEs, with a MAE of 310.9 cm^{-1}, relative to the other F12+EOM QFFs, despite slightly outperforming them for fundamental frequencies. Possibly, the shape of the potential energy surface computed by F12+EOM-DZ is more accurate, despite having a less accurate adiabatic excitation energy, resulting in more accurate frequencies. Thus, the cost-savings of the double-zeta basis set may be useful when only fundamental frequencies

are needed, but triple-zeta quality may be necessary for these methods if accurate AEEs are desired.

The average error for AEEs for (T)+EOM/CcCR are similar to F12+EOM-TZ and F12cCR+EOM. Looking only at the average ΔAEE may be somewhat misleading as the AEEs for the individual molecules differ somewhat dramatically between methods. For example, the computed ΔAEE versus experiment for HNCO is 631.5 cm^{-1} for F12+EOM-TZ and 1059.3 cm^{-1} for (T)+EOM/CcCR. Notably, (T)+EOM/CcCR achieves the closest AEEs to experimental values for all molecules except HOO and HNCO, where larger errors bias the average result.

Figure 1 gives mean absolute percent error (MA%E) for F12+EOM-TZ, F12cCR+EOM and (T)+EOM/CcCR compared to experimental vibrational frequencies. Additionally, this figure provides average walltimes for each QFF relative to (T)+EOM/CcCR walltime. F12+EOM-DZ is omitted from this figure as these computations were run on a different cluster than the others, thus direct walltime comparisons cannot be made for this method. Average MA%Es are 2.4 %, 2.5 % and 2.6% for F12+EOM-TZ, F12cCR+EOM and (T)+EOM/CcCR, respectively. These differences are relatively small. Thus, based on this data, the choice of method among these three does not appear to have much effect on accuracy compared to experiment.

In looking at timings, the walltimes for both methods are a small fraction of the (T)+EOM/CcCR walltime. F12+EOM-TZ is about 70 times faster, whlie F12-TZ-cCR is about 19 times faster. It should be cautioned that these timings are approximate, as they use walltime rather than CPU time and are somewhat confounded by the use of different quantum chemistry packages. However, they should be useful as qualitative guidelines, and it should be *a priori* evident that F12+EOM-TZ and F12cCR+EOM will be significantly faster due to the reduced basis set size. Differences in timings would also be expected to become more exaggerated with larger systems due to exponential scaling. So far, it seems reasonable to estimate that F12+EOM-TZ and F12cCR+EOM are strict improvements over (T)+EOM/CcCR. The

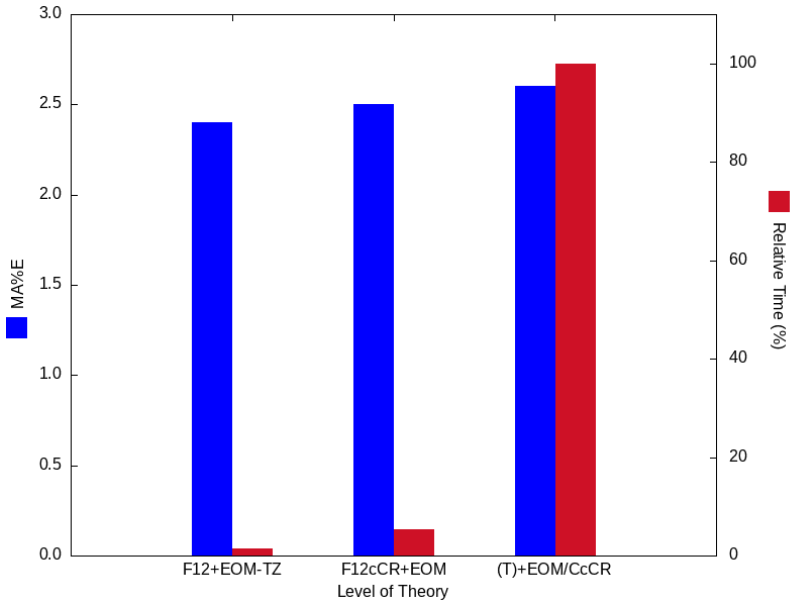

Figure 1: F12+EOM, F12cCR+EOM and (T)+EOM/CcCR mean absolute percent error (MA%E) compared to experimental values (blue) together with walltimes as a percentage of (T)+EOM/CcCR walltime (red)

choice between F12+EOM-TZ and F12cCR+EOM is somewhat more nebulous, although the additional corrective terms in the latter would, at least naively, be expected to produce more accurate rotational constants in cases where the two differ significantly. Overall, experimental comparisons suggest that the F12+EOM family of QFFs are achieving their goal of greatly reducing computational cost from the similar (T)+EOM method by taking advantage of explicitly correlated methods.

Theoretical comparisons

Table 3: Mean Absolute Differences for Vibrational Frequencies of Electronically Excited State QFFs versus Ground State-type Benchmark QFFs in cm^{-1}

Excited State Method		F12+EOM-DZ			F12+EOM-TZ			F12cCR+EOM			(T)+EOM/CcCR	
Ground State Method	vs F12-TZ	vs F12-TZ-cCR	vs CcCR	vs F12-TZ	vs F12-TZ-cCR	vs CcCR	vs F12-tZ	vs F12-TZ-cCR	vs CcCR	vs F12-TZ	vs F12-TZ-cCR	vs CcCR
A $^2A'$ HNF	11.1	9.3	8.6	2.4	2.5	3.0	4.4	0.7	0.9	6.9	10.3	10.0
A $^2A'$ HSO	10.0	8.1	75.3	1.5	2.3	77.8	2.2	0.7	76.7	2.3	3.9	77.9
A $^2A'$ HSS	4.9	3.6	3.4	2.1	3.3	4.7	3.0	4.2	5.8	3.2	4.4	4.4
A $^2A'$ HOO	7.4	8.7	15.1	2.3	2.8	12.5	18.7	16.7	9.3	1.7	1.5	13.2
average	8.3	7.4	25.6	2.1	2.7	24.5	7.1	5.6	23.2	3.5	5.0	26.4

Table 3 gives comparisons of the (T)+EOM/CcCR, F12+EOM-DZ, F12+EOM-TZ, and F12cCR+EOM QFFs to F12-TZ, F12-TZ-cCR and CcCR ground state benchmarks for $\tilde{A}\ ^2A'$ HNF, $\tilde{A}\ ^2A'$ HSO, $\tilde{A}\ ^2A'$ HSS, and $\tilde{A}\ ^2A'$ HOO. These ground state type QFFs routinely compute vibrational frequencies within 5 cm^{-1} of experiment,[11,13–24,27–30] motivating their usage as theoretical benchmarks here. F12+EOM-TZ approximates F12-TZ well for these states with the total average of mean absolute differences (MAD) of 2.1 cm^{-1}. F12-TZ-cCR is also approximated well with a MAD of 2.7 cm^{-1} between F12+EOM-TZ and F12-TZ-cCR. F12cCR+EOM performs a bit less well with MADs of 7.1 and 5.6 cm^{-1}, respective of F12-TZ and F12-TZ-cCR. This is mostly due to disagreement with the ν_2 mode (the O–O stretch) of HOO, which has a difference of 35.1 cm^{-1} between F12cCR+EOM and F12-TZ. Similar issues have been seen previously with MOLPRO predictions[36] for this mode. Hence, this behavior may be anomalous rather than a systemic flaw with the approach. F12+EOM-DZ performs less well compared to these theoretical benchmarks than for the experimental benchmarks given above. The average MAD for F12+EOM-DZ compared to F12-TZ is 8.3, while the average MAD is 7.4 compared to F12-TZ-cCR. The MADs are higher than F12+EOM-TZ for all four molecules in Table 3, so the higher average is not because of a major outlier. Possibly, F12+EOM-DZ outperforming F12+EOM-TZ for experimental benchmarks is fortuitous, as one would expect a lower quality basis set to give lower quality results, as seen in Table 3.

F12+EOM-TZ agrees better with the benchmark QFFs than (T)+EOM/CcCR does. F12+EOM-TZ and F12-TZ both rely on CCSD(T)-F12/cc-pVTZ-F12 energies, so this is a fairly predictable outcome. Considering, though, the robust performance of F12-TZ,[24] F12+EOM-TZ's close agreement with the former benchmark suggests that the F12+EOM-TZ approach will be valuable in cases where F12-TZ cannot be trivially applied as in the case of variationally-accessible electronic states. Additionally, (T)+EOM/CcCR and F12+EOM-TZ do not deviate much from the benchmarks, with (T)+EOM/CcCR only about 2 cm^{-1} higher in MAD meaning that there may be little practical difference between the methods in

terms of their produced spectroscopic data. F12+EOM-DZ, however, underperforms when compared to (T)+EOM/CcCR. Thus, the cost-savings from dropping to the double-zeta basis set may not be worthwhile based on the current theoretical comparisons.

All four QFFs compare somewhat poorly with the CcCR reference QFF. Although CcCR can produce quite accurate constants, it can be unreliable in some cases, such as in bonds with flat potentials.[77] In particular, CcCR deviates significantly for HSO, potentially indicating problems describing sulfurous bonds or perhaps S–O bonds in particular. This may be due to the highly composite nature of CcCR resulting in some numerical instability, or perhaps in its treatment of core correlation. Larger QFF step sizes may also be necessary to account for proper treatment of sulfur-containing species.[30] Owing to these considerations and the discrepancies with the F12-TZ and F12-TZ-cCR results, the problem with the CcCR references are likely due to flaws with the latter for these systems.

Table 4: Mean Absolute Differences for Rotational Constants of Electronically Excited State QFFs versus Ground State-type Benchmark QFFs in MHz

Excited State Method		F12+EOM-DZ			F12+EOM-TZ			F12cCR+EOM			(T)+EOM/CcCR		
Ground State Method	Constant	vs F12-TZ	vs F12-TZ-cCR	vs CcCR	vs F12-TZ	vs F12-TZ-cCR	vs CcCR	vs F12-tZ	vs F12-TZ-cCR	vs CcCR	vs F12-TZ	vs F12-TZ-cCR	vs CcCR
A $^2A'$ HNF	A	14509	10985	8484	4903	2440	2423	8858	5335	3313	6442	3101	2105
	B/ C	42	108	138	30	95	126	29	37	67	54	12	42
A $^2A'$ HSO	A	2028	1704	9220	284	80	10965	540	216	10709	244	80	11004
	B/ C	117	87	8363	27	4	8453	28	6	8452	20	9	8460
A $^2A'$ HSS	A	1636	1249	997	132	254	506	27	402	654	474	88	165
	B/ C	12	14	35	1	25	46	18	8	29	37	11	10
A $^2A'$ HOO	A	860	312	1573	97	1251	2513	656	516	1778	1825	653	609
	B/ C	136	195	261	53	112	178	2	59	125	51	8	74
average	A	4758	3563	5069	1354	1006	4102	2520	1617	4113	2246	980	3471
average	B / C	77	101	2199	28	59	2201	19	27	2168	41	10	2146

Table 4 compares the rotational constants for these levels of theory. In keeping with previous QFF work,[30] the A and B/C rotational constants are analyzed separately, as the former typically has much greater variation between methods and more difficulty in matching experiment. Looking at the B and C rotational constants, F12+EOM-TZ compares to within a 28 MHz MAD (0.11 %) of F12-TZ. The comparison with F12-TZ-cCR is also favorable with an MAD of 59 MHz (0.27 %). The small difference here is noteworthy, as the core correlation included in F12-TZ-cCR is generally necessary for accurate rotational constants. However, it must be cautioned that this close matching may not extrapolate beyond this small test set. The difference observed for the A rotational constants is quite a bit larger at about 1000 MHz compared to both F12-TZ and F12-TZ-cCR. As noted, this is to be expected. F12+EOM-DZ differs dramatically from F12+EOM-TZ in the rotational constants, with an average MAD of 4758 MHz for the A rotational constant. This result is in line with the sub-par performance of this method for theoretical benchmarks of fundamental vibrational frequencies. The difference is, however, less severe in the B and C rotational constants, where the MAD for F12+EOM-DZ versus F12-TZ is only 77 MHz, though this is still higher than the average MAD observed with F12+EOM-TZ at 28 MHz versus F12-TZ.

F12cCR+EOM sees similarly close agreement to F12-TZ and F12-TZ-cCR in the B and C rotational constants, with an MAD of 27 MHz between F12cCR+EOM and F12-TZ-cCR. The A rotational constants differ somewhat more, with MADs of 2520 MHz vs F12-TZ and 1617 MHz vs F12cCR. As is shown for the vibrational frequencies, CcCR disagrees with the other two benchmark QFFs. This is particularly true, again, for HSO, which may be due to similar issues as outlined above with the fundamental vibrational frequencies. Without experimental comparisons, knowing which QFF best approximates the "correct" answer is difficult. However, rotational constants are quite difficult to obtain for electronically excited states making theory to theory benchmarks necessary.

Again, as with vibrational frequencies, F12+EOM-TZ and F12cCR+EOM perform as well or better than (T)+EOM/CcCR compared to these ground-state type benchmarks. Al-

though (T)+EOM/CcCR may ostensibly be a higher level of theory, as it includes a complete basis set extrapolation along with core correlation and scalar relativistic effects, this method is not necessarily more trustworthy. It likely has the same numerical stability problems as its parent CcCR approach, compounded by the composite (T)+EOM energy. F12cCR+EOM, by comparison, accounts for many of the same effects but with significantly less individual terms: 14 total terms for (T)+EOM–7 each for CCSD(T) and EOM-CCSD components– compared to 6 total for F12cCR+EOM. Because of these considerations, (T)+EOM/CcCR lacks a clear competitive advantage based on the present theory to theory comparisons. F12+EOM-DZ performs well for experimental comparisons of fundamental vibrational frequencies, but lags behind the other F12+EOM QFFs for experimental AEE comparisons as well as theoretical benchmarks of vibrational frequencies and rotational constants. Thus, it appears that F12+EOM-DZ cannot confidently be recommended over F12+EOM-TZ, unless the triple-zeta basis set of F12+EOM-TZ is computationally infeasible for a given system.

Overall, theoretical and experimental benchmarks lead to the same conclusions: there is no clear, unambiguous superiority in accuracy between F12+EOM-TZ, F12cCR+EOM and (T)+EOM/CcCR. As such and since the former are much less computationally costly owing to decreased basis set size, they are recommended for use. Although F12+EOM-TZ makes up for the smaller basis set size with explicit correlation, this is not accounted in the EOM-CCSD/aug-cc-pVTZ portion of the total energy. This seems not to make much difference with vibrational frequencies but may be responsible for somewhat worse performance in computing AEEs. A potential improvement would be to use some perturbative-triples containing EOM approach, such as EOM-CCSD(T),[78] but none of these have been standardized and adopted by the community in the same way that ground state CCSD(T) has. Analysis of such methods is left for future work.

Conclusions

The F12+EOM-TZ and F12cCR+EOM QFFs defined and explored in this work seem to be clear improvements on the previous (T)+EOM/CcCR method mainly since they are orders of magnitude faster for similar performance in comparison to theoretical and experimental benchmarks. They compare quite well with theoretical benchmarks, with F12+EOM comparing to within less than 3 cm^{-1} MAD of its F12-TZ cousin for fundamental vibrational frequencies. B and C rotational constants are also very well behaved (0.12 MA%D for F12cCR+EOM vs F12-TZ-cCR) with A rotational constants showing a somewhat larger difference of about 1000 MHz.

F12cCR+EOM performs quite similarly to F12+EOM-TZ. This method has more theory included within its framework accounting for core correlation as well as scalar relativistic effects. However, it remains unclear if this results in a superior QFF since there may be resultant issues in numerical stability. The increased computational cost may be non-negligible for larger systems with many core electrons. Future applications of these methods should help determine which is the superior option, in, general, or if the choice should be made on a case-by-case basis or if it matters at all. The F12+EOM-DZ QFF performs well compared to experimental benchmarks for vibrational frequencies with an average MAD of 35.5 cm^{-1}, although it does not perform as well for theoretical benchmarks or for experimental comparisons of AEEs. The double-zeta basis set means this QFF may be useful for larger systems where the triple-zeta basis set of the F12+EOM-TZ is not feasible, however the present data suggests it may be less trustworthy.

In conclusion, F12+EOM-TZ and/or F12cCR+EOM should be preferentially used over (T)+EOM/CcCR in exploring the potential and application of this family of electronically excited state QFF approaches. The present work does not prescribe these as a proverbial "silver bullet" for spectroscopic data of electronically excited states as the test cases studied herein are of limited scope and number, but they show promise as an avenue worthy of future exploration. More work should be done exploring applicability to multiple categories

of electronically excited states. Application is also likely limited to reasonably well behaved states dominated by single excitations, owing to the reliance on EOM-CCSD energies, but this still likely represents a majority of uses for this method.

Overall, the increased speed of the F12+EOM-TZ and F12cCR+EOM approaches should open the door to exploration of electronically excited state QFFs for larger molecules. These methods may be potent tools for "pulling the weeds" of astronomical spectra and for enhanced quantum chemical understanding of many important electronic transitions and states.

Acknowledgement

Funding is acknowledged from NSF grant OIA-1757220, NASA grant NNX17AH15G, and start-up funds provided by the University of Mississippi. Additionally, the computing resources were provided in part by the Mississippi Center for Supercomputing Research funded with contributions from NSF grant CHE-1757888.

Supporting Information Available

Supplementary information contains full harmonic and fundamental vibrational frequencies computed in this work and experimental references used, as well as rotational constants.

References

(1) Dreuw, A.; Head-Gordon, M. Single-Reference *ab initio* Methods for the Calculation of Excited States of Large Molecules. *Chem. Rev.* **2005**, *105*, 4009–4037, PMID: 16277369.

(2) González, L.; Escudero, D.; Serrano-Andrés, L. Progress and Challenges in the Calculation of Electronic Excited States. *ChemPhysChem* **2012**, *13*, 28–51.

(3) Fortenberry, R. C. Quantum Astrochemical Spectroscopy. *Int. J. Quant. Chem.* **2017**, *117*, 81–91.

(4) Fortenberry, R. C.; Bodewits, D.; Pierce, D. M. Knowledge Gaps in the Cometary Spectra of Oxygen-Bearing Molecular Cations. *Astrophys. J., Suppl. Ser.* **2021**, *256*, 6.

(5) Hänni, N.; Altwegg, K.; Combi, M.; Fuselier, S. A.; Keyser, J. D.; Rubin, M.; Wampfler, S. F. Identification and characterization of a new ensemble of cometary organic molecules. *Nat. Commun.* **2022**, *13*.

(6) Bodewits, D. et al. Changes in the Physical Environment of the Inner Coma of 67P/Churyumov-Gerasimenko with Decreasing Heliocentric Distance. *Astron. J.* **2016**, *152*, 130.

(7) Fortman, S. M.; Medvedev, I. R.; Neese, C. F.; Lucia, F. C. D. How Complete are Astrophysical Catalogs for the Millimeter and Submillimeter Spectral Region? *Astrophys. J.* **2010**, *725*, l11–l14.

(8) Raghavachari, K.; Trucks, G. W.; Pople, J. A.; Head-Gordon, M. A Fifth-Order Perturbation Comparison of Electron Correlation Theories. *Chem. Phys. Lett.* **1989**, *157*, 479–483.

(9) Shavitt, I.; Bartlett, R. J. *Many-Body Methods in Chemistry and Physics: MBPT and Coupled-Cluster Theory*; Cambridge University Press: Cambridge, 2009.

(10) Crawford, T. D.; Schaefer III, H. F. In *Rev. Comput. Chem.*; Lipkowitz, K. B., Boyd, D. B., Eds.; Wiley: New York, 2000; Vol. 14; pp 33–136.

(11) Fortenberry, R. C.; Lee, T. J. Computational Vibrational Spectroscopy for the Detection of Molecules in Space. *Ann. Rep. Comput. Chem.* **2019**, *15*, 173–202.

(12) Huang, X.; Valeev, E. F.; Lee, T. J. Comparison of One-Particle Basis Set Extrapolation to Explicitly Correlated Methods for the Calculation of Accurate Quartic Force Fields,

Vibrational Frequencies, and Spectroscopic Constants: Application to H_2O, N_2H^+, NO_2^+, and C_2H_2. *J. Chem. Phys.* **2010**, *133*, 244108.

(13) Huang, X.; Taylor, P. R.; Lee, T. J. Highly Accurate Quartic Force Field, Vibrational Frequencies, and Spectroscopic Constants for Cyclic and Linear $C_3H_3^+$. *J. Phys. Chem. A* **2011**, *115*, 5005–5016.

(14) Fortenberry, R. C.; Huang, X.; Francisco, J. S.; Crawford, T. D.; Lee, T. J. Quartic Force Field Predictions of the Fundamental Vibrational Frequencies and Spectroscopic Constants of the Cations $HOCO^+$ and $DOCO^+$. *J. Chem. Phys.* **2012**, *136*, 234309.

(15) Fortenberry, R. C.; Huang, X.; Francisco, J. S.; Crawford, T. D.; Lee, T. J. Fundamental Vibrational Frequencies and Spectroscopic Constants of $HOCS^+$, $HSCO^+$, and Isotopologues via Quartic Force Fields. *J. Phys. Chem. A.* **2012**, *116*, 9582–9590.

(16) Zhao, D.; Doney, K. D.; Linnartz, H. Laboratory Gas-Phase Detection of the Cyclopropenyl Cation (c-$C_3H_3^+$). *Astrophys. J. Lett.* **2014**, *791*, L28.

(17) Morgan, W. J.; Fortenberry, R. C. Theoretical Rovibronic Treatment of the $\tilde{X}^2\Sigma^+$ and $^2\Pi$ States of C_2H & $^1\Sigma^+$ State of C_2H^- from Quartic Force Fields. *J. Phys. Chem. A* **2015**, *119*, 7013–7025.

(18) Theis, R. A.; Fortenberry, R. C. Potential Interstellar Noble Gas Molecules: $ArOH^+$ and $NeOH^+$ Rovibrational Analysis from Quantum Chemical Quartic Force Fields. *Molec. Astrophys.* **2016**, *2*, 18–24.

(19) Bizzocchi, L.; Lattanzi, V.; Laas, J.; Spezzano, S.; Giuliano, B. M.; Prudenzano, D.; Endres, C.; Sipilä, O.; Caselli, P. Accurate Sub-millimetre Rest Frequencies for $HOCO^+$ and $DOCO^+$ Ions. *Astron. Astrophys.* **2017**, *602*, A34.

(20) Kitchens, M. J. R.; Fortenberry, R. C. The Rovibrational Nature of Closed-Shell Third-

Row Triatomics: HOX and HXO, X = Si^+, P, S^+, and Cl. *Chem. Phys.* **2016**, *472*, 119–127.

(21) Fortenberry, R. C.; Francisco, J. S. On the Detectability of the $\tilde{X}\ ^2A''$ HSS, HSO, and HOS Radicals in the Interstellar Medium. *Astrophys. J.* **2017**, *835*, 243.

(22) Fuente, A.; Goicoechea, J. R.; Pety, J.; Gal, R. L.; Martín-Domńech, R.; Gratier, P.; Guzmán, V.; Roueff, E.; Loison, J. C.; Caro, G. M. M. o.; Wakelam, V.; Gerin, M.; Riviere-Marichalar, P.; Vidal, T. First Detection of Interstellar S_2H. *Astrophys. J. Lett* **2017**, *851*, 49.

(23) Wagner, J. P.; McDonald II, D. C.; Duncan, M. A. An Argon–Oxygen Covalent Bond in the $ArOH^+$ Molecular Ion. *Angew. Chem. Int. Ed* **2018**, *57*, 5081–5085.

(24) Gardner, M. B.; Westbrook, B. R.; Fortenberry, R. C.; Lee, T. J. Highly-Accurate Quartic Force Fields for the Prediction of Anharmonic Rotational Constants and Fundamental Vibrational Frequencies. *Spectrochim. Acta A* **2021**, *248*, 119184.

(25) Adler, T. B.; Knizia, G.; Werner, H.-J. A Simple and Efficient CCSD(T)-F12 Approximation. *J. Chem. Phys.* **2007**, *127*, 221106.

(26) Knizia, G.; Adler, T. B.; Werner, H.-J. Simplified CCSD(T)-F12 Methods: Theory and Benchmarks. *J. Chem. Phys.* **2009**, *130*, 054104.

(27) Agbaglo, D.; Lee, T. J.; Thackston, R.; Fortenberry, R. C. A Small Molecule with PAH Vibrational Properties and a Detectable Rotational Spectrum: *c*-$(C)C_3H_2$, Cyclopropenylidenyl Carbene. *Astrophys. J.* **2019**, *871*, 236.

(28) Agbaglo, D.; Fortenberry, R. C. The Performance of CCSD(T)-F12/aug-cc-pVTZ for the Computation of Anharmonic Fundamental Vibrational Frequencies. *Int. J. Quantum Chem.* **2019**, *119*, e25899.

(29) Agbaglo, D.; Fortenberry, R. C. The Performance of Explicitly Correlated Wavefunctions [CCSD(T)-F12b] in the Computation of Anharmonic Vibrational Frequencies. *Chem. Phys. Lett.* **2019**, *734*, 136720.

(30) Watrous, A. G.; Westbrook, B. R.; Fortenberry, R. C. F12-TZ-cCR: A Methodology for Faster and Still Highly Accurate Quartic Force Fields. *J. Phys. Chem. A* **2021**, *125*, 10532–10540.

(31) Morgan, W. J.; Fortenberry, R. C. Quartic Force Fields for Excited Electronic States: Rovibronic Reference Data for the 1 $^2A'$ and 1 $^2A''$ States of the Isoformyl Radical, HOC. *Spectrochim. Acta A* **2015**, *135*, 965–972.

(32) Fortenberry, R. C.; Trabelsi, T.; Francisco, J. S. Hydrogen Sulfide as a Scavenger of Sulfur Atomic Cation. *J. Phys. Chem. A* **2018**, *122*, 4983–4987.

(33) Stanton, J. F.; Bartlett, R. J. The Equation of Motion Coupled-Cluster Method - A Systematic Biorthogonal Approach to Molecular Excitation Energies, Transition-Probabilities, and Excited-State Properties. *J. Chem. Phys.* **1993**, *98*, 7029–7039.

(34) Fortenberry, R. C.; King, R. A.; Stanton, J. F.; Crawford, T. D. A Benchmark Study of the Vertical Electronic Spectra of the Linear Chain Radicals C_2H and C_4H. *J. Chem. Phys.* **2010**, *132*, 144303.

(35) Matthews, D. A. EOM-CC methods with Approximate Triple Excitations Applied to Core Excitation and Ionisation Energies. *Mol. Phys.* **2020**, *118*, e1771448.

(36) Davis, M. C.; Fortenberry, R. C. (T)+EOM Quartic Force Fields for Theoretical Vibrational Spectroscopy of Electronically Excited States. *J. Chem. Theory Comput.* **2021**, *17*, 4374–4382.

(37) Györffy, W.; Werner, H.-J. Analytical Energy Gradients for Explicitly Correlated Wave

Functions. II. Explicitly Correlated Coupled Cluster Singles and Doubles with Perturbative Triples Corrections: CCSD(T)-F12. *J. Chem. Phys.* **2018**, *148*, 114104.

(38) Krylov, A. I. Equation-of-Motion Coupled Cluster Methods for Open-Shell and Electronically Excited Species: The Hitchiker's Guide to Fock Space. *Ann. Rev. Phys. Chem.* **2007**, *59*, 433–463.

(39) Krylov, A. *Reviews in Computational Chemistry*; John Wiley & Sons, Ltd, 2017; Chapter 4, pp 151–224.

(40) Jungen, C. The Renner-Teller Effect Revisited 40 Years Later. *J. Mol. Spectrosc.* **2019**, *363*, 111172.

(41) McGuire, B. A. 2018 Census of Interstellar, Circumstellar, Extragalactic, Protoplanetary Disk, and Exoplanetary Molecules. *Astrophys. J. Suppl. Ser.* **2018**, *239*, 17.

(42) Parise, B.; Bergman, P.; Du, F. Detection of the Hydroperoxyl Radical HO_2 toward ρ_o Ophiuchi A. Addtional Constraints on the Water Chemical Network. *Astron. Astrophys.* **2012**, *541*, L11.

(43) Huber, K. P.; Herzberg, G.; Gallagher, J. W.; Johnson, R. D. In *Constants of Diatomic Molecules*; Linstrom, P. J., Mallard, W. G., Eds.; National Institute of Standards and Technology: Gaithersburg MD, 2018; p 69.

(44) Gaw, J. F.; Willets, A.; Green, W. H.; Handy, N. C. In *Advances in Molecular Vibrations and Collision Dynamics*; Bowman, J. M., Ratner, M. A., Eds.; JAI Press, Inc.: Greenwich, Connecticut, 1991; pp 170–185.

(45) Watson, J. K. G. In *Vibrational Spectra and Structure*; During, J. R., Ed.; Elsevier: Amsterdam, 1977; pp 1–89.

(46) Papousek, D.; Aliev, M. R. *Molecular Vibration-Rotation Spectra*; Elsevier: Amsterdam, 1982.

(47) Martin, J. M. L.; Taylor, P. R. Accurate *ab Initio* Quartic Force Field for *trans*-HNNH and Treatment of Resonance Polyads. *Spectrochim. Acta A* **1997**, *53*, 1039–1050.

(48) Hill, J. G.; Peterson, K. A. Correlation Consistent Basis Sets for Explicitly Correlated Wavefunctions: Valence and Core-Valence Basis Sets for Li, Be, Na, and Mg. *Phys. Chem. Chem. Phys.* **2010**, *12*, 10460–10468.

(49) Douglas, M.; Kroll, N. Quantum Electrodynamical Corrections to the Fine Structure of Helium. *Ann. Phys.* **1974**, *82*, 89–155.

(50) Jansen, G.; Hess, B. A. Revision of the Douglas-Kroll Hamiltonian. *Phys. Rev. A* **1989**, *39*, 6016–6017.

(51) Dunning, T. H. Gaussian Basis Sets for Use in Correlated Molecular Calculations. I. The Atoms Boron through Neon and Hydrogen. *J. Chem. Phys.* **1989**, *90*, 1007–1023.

(52) Kendall, R. A.; Dunning, T. H.; Harrison, R. J. Electron Affinities of the First-Row Atoms Revisited. Systematic Basis Sets and Wave Functions. *J. Chem. Phys.* **1992**, *96*, 6796–6806.

(53) Peterson, K. A.; Dunning, T. H. Benchmark Calculations with Correlated Molecular Wave Functions. VII. Binding Energy and Structure of the HF Dimer. *J. Chem. Phys.* **1995**, *102*, 2032–2041.

(54) Martin, J. M. L.; Taylor, P. R. Basis Set Convergence for Geometry and Harmonic Frequencies. Are *h* Functions Enough? *Chem. Phys. Lett.* **1994**, *225*, 473–479.

(55) Fortenberry, R. C.; Huang, X.; Francisco, J. S.; Crawford, T. D.; Lee, T. J. The *trans*-HOCO Radical: Fundamental Vibrational Frequencies, Quartic Force Fields, and Spectroscopic constants. *J. Chem. Phys.* **2011**, *135*, 134301.

(56) Werner, H.-J. et al. The Molpro Quantum Chemistry Package. *J. Chem. Phys.* **2020**, *152*, 144107.

(57) Parrish, R. M. et al. Psi4 1.1: An Open-Source Electronic Structure Program Emphasizing Automation, Advanced Libraries, and Interoperability. *J. Chem. Theory Comput.* **2017**, *13*, 3185–3197.

(58) Liu, W.; Peng, D. Exact two-component Hamiltonians revisited. *J. Chem. Phys.* **2009**, *131*, 031104.

(59) Hunziker, H. E.; Wendt, H. R. Electronic Absorption Spectra of Organic Peroxyl Radicals in the Near Infrared. *J. Chem. Phys.* **1976**, *64*, 3488–3490.

(60) Becker, K. H.; Fink, E. H.; Leiss, A.; Schurath, U. A Study of the Near Infrared Emission Bands of the Hydroperoxyl Radical at Medium Resolution. *Chem. Phys. Lett.* **1978**, *54*, 191–196.

(61) Fink, E. H.; Kruse, H.; Ramsay, D. A. Paper WF2, 42nd Symposium on Molecular Spectroscopy. Columbus, Ohio, 1987.

(62) Woodman, C. M. The absorption spectrum of HNF in the region 3800–5000 Å. *J. Mol. Spectrosc.* **1970**, *33*, 311–344.

(63) Jacox, M. E.; Milligan, D. E. Production and Reaction of Atomic Fluorine in Solids. Vibrational and Electronic Spectra of the Free Radical HNF. *J. Phys. Chem.* **1967**, *46*, 184–191.

(64) Merer, A. J.; Travis, D. N. Rotational Analysis of Bands of the HCF Molecule. *Can. J. Phys.* **1966**, *44*, 1541–1550.

(65) Schmidt, T. W.; Bacskay, G. B.; Kable, S. H. Characterization of the $\tilde{A}(^1A'')$ state of HCF by laser induced fluorescence spectroscopy. *J. Chem. Phys.* **1999**, *110*, 11277–11285.

(66) Nauta, K.; Guss, J. S.; Owens, N. L.; Kable, S. H. Reassignment of the CH stretching frequency of CHF in the $\tilde{A}$ electronic state. *J. Chem. Phys.* **2004**, *120*, 3517–3518.

(67) Fan, H.; Mukarakate, C.; Deselnicu, M.; Tao, C.; Reid, S. A. Dispersed Fluorescence Spectroscopy of Jet-Cooled HCF and DCF: Vibrational Structure of the $\tilde{\mathrm{X}}\ ^1\mathrm{A}'$ State. *J. Chem. Phys.* **2005**, *123*, 014314.

(68) Hakuta, K. Vibration-Rotation Spectrum of HCF ($\tilde{\mathrm{X}}\ ^1\mathrm{A}'$) by Laser-Induced Fluorescence. *J. Mol. Spetrosc.* **1984**, *106*, 56–63.

(69) Dalby, F. W. The Spectrum and Structure of the HNO Molecule. *Can. J. Phys.* **1958**, *36*, 1336–1371.

(70) Bancroft, J. L.; Hollas, J. M.; Ramsay, D. A. The Absorption Spectra of HNO and DNO. *Can. J. Phys.* **1962**, *40*, 322–347.

(71) Schurath, U.; Weber, M.; Becker, K. H. Electronic spectrum and structure of the HSO radical. *J. Chem. Phys.* **1977**, *67*, 110–119.

(72) Holstein, K. J.; Find, E. H.; Wildt, J.; Zabel, F. The $\tilde{\mathrm{A}}\ ^2A' \leftarrow \tilde{\mathrm{X}}\ ^2A''$ Emission Spectrum of the HS_2 Radical. *Chem. Phys. Lett.* **1985**, *113*, 1–7.

(73) Ashworth, S. H.; Fink, E. H. The high resolution Fourier-transform chemiluminescence spectrum of the HS_2 radical. *Mol. Phys.* **2007**, *105*, 715–725.

(74) Entfellner, M.; Boesl, U. Photodetachment-photoelectron spectroscopy of disulfanide: the ground and first excited electronic state of HS_2 and DS_2. *Phys. Chem. Chem. Phys.* **2009**, *11*, 2657.

(75) Dixon, R. N.; Kirby, G. H. Ultra-violet absorption spectrum of isocyanic acid. *Transactions of the Faraday Society* **1968**, *64*, 2002.

(76) Berghout, H. L.; Crim, F. F.; Zyrianov, M.; Reisler, H. The electronic origin and vibrational levels of the first excited singlet state of isocyanic acid (HNCO). *J. Chem. Phys.* **2000**, *112*, 6678–6688.

(77) Trabelsi, T.; Davis, M. C.; Fortenberry, R. C.; Francisco, J. S. Spectroscopic Investigation of [Al,N,C,O] Refractory Molecules. *J. Chem. Phys.* **2019**, *151*, 244303.

(78) Watts, J. D.; Bartlett, R. J. Economical Triple Excitation Equation-of-Motion Coupled-Cluster Methods for Excitation Energies. *Chem. Phys. Lett.* **1995**, *233*, 81–87.